In Vitro Cell.Dev.Biol.—Animal
DOI 10.1007/s11626-016-0039-8

# Heat shock protein 70 inhibits cardiomyocyte necroptosis through repressing autophagy in myocardial ischemia/reperfusion injury

Xiaojuan Liu[1,2] · Chao Zhang[2,3] · Chi Zhang[2,3] · Jingjing Li[2,3] · Wanwan Guo[2,3] · Daliang Yan[2,4] · Chen Yang[2,4] · Jianhua Zhao[2,4] · Tian Xia[1] · Yuqing Wang[1] · Rong Xu[1] · Xiang Wu[2,3] · Jiahai Shi[2,4]

Received: 24 January 2016 / Accepted: 5 April 2016 / Editor: Tetsuji Okamoto


**Abstract** Irreversible damage of cardiac function arisen from myocardial ischemia/reperfusion injury (MIRI) leads to an emerging challenge in the treatments of cardiac ischemic diseases. Molecular chaperone heat shock protein 70 (HSP70) attenuates heat-stimulated cell autophagy, apoptosis, and damage in the heart. Under specific conditions, autophagy may, directly or indirectly, induce cell death including necroptosis. Whether HSP70 inhibits cardiomyocyte necroptosis via suppressing autophagy during MIRI is unknown. In our study, HSP70 expression was opposite to necroptosis marker RIP1 and autophagy marker LC3A/B expression after myocardial ischemia/reperfusion (MIR) in vivo. Furthermore, in vitro primary rat cardiomyocytes mimicked MIRI by hypoxia/reoxygenation (H/R) treatment. Knockdown of HSP70 expression promoted cardiomyocyte autophagy and necroptosis following H/R treatment, while the increase tendency was downregulated by autophagy inhibitor 3-MA, showing that autophagy-induced necroptosis could be suppressed by HSP70. In summary, HSP70 downregulates cardiomyocyte necroptosis through suppressing autophagy during myocardial IR, revealing the novel protective mechanism of HSP70 and supplying a novel molecular target for the treatment of heart ischemic diseases.

**Keywords** HSP70 · Autophagy · Necroptosis · Myocardial ischemia/reperfusion injury

## Introduction

Myocardial infarction is the result of coronary artery occlusion which contributes to the high mortality around the world. The loss of blood flow may lead to the death of cardiomyocytes in the ischemia region (Murphy and Steenbergen 2008; Rafiq *et al.* 2014). With the early recovery of the arterial blood flow, a controversial injury caused by reperfusion has been arisen as a novel topic during the treatment of ischemic heart diseases, which limits the efficiency of vascular recanalization such as percutaneous coronary intervention and thrombolysis medicine applications (Vander Heide and Steenbergen 2013; Matsushima *et al.* 2014). MIRI triggers a complex reaction of cardiac tissue, which results in cardiomyocyte death (Whelan *et al.* 2010). It is of great significance that the underlying mechanism of MIRI is a systematic network with a various number of pathophysiological process and numerous molecules (Gottlieb *et al.* 2009). To abolish the negative effect of this pathophysiological process, researchers found heat shock protein 70 (HSP70) was protective during MIRI, which was a promising target for clinical treatments (Garrido *et al.* 2006; Feng *et al.* 2014; Vicencio *et al.* 2015).

Xiaojuan Liu, Chao Zhang, Xiang Wu and Jiahai Shi contributed equally to this work.

✉ Xiang Wu
ntwx0513@163.com

✉ Jiahai Shi
ntsjh0513@163.com

[1] Department of Pathogen Biology, Medical College, Nantong University, Nantong, Jiangsu 226001, People's Republic of China

[2] Jiangsu Province Key Laboratory for Inflammation and Molecular Drug Target, Medical College, Nantong University, Nantong, Jiangsu 226001, People's Republic of China

[3] Department of Cardiology, Affiliated Hospital of Nantong University, Nantong 226001, People's Republic of China

[4] Department of Thoracic Surgery, Affiliated Hospital of Nantong University, Nantong, Jiangsu 226001, People's Republic of China

Published online: 29 April 2016

HSP70 is regarded as cardiac protective molecules and could be upregulated to inhibit cardiomyocyte apoptosis after MIR (Peng *et al.* 2010). In addition, overexpression of HSP70 could inhibit caspase-dependent cardiomyocyte apoptosis which significantly improves the cardiac function (Rani *et al.* 2013). Besides inhibition of apoptosis (Sun *et al.* 2015), HSP70 was recently proven to attenuate cell death and autophagy via reducing LC3B expression during heat shock response (Hsu *et al.* 2013). Autophagy, which can induce necroptosis, plays a detrimental role during MIRI (Huang *et al.* 2015; Jiang *et al.* 2015). Necroptosis, a programmed necrosis, triggers a variety of reactions enhancing cellular death during stress exposure (Dannappel *et al.* 2014; Koshinuma *et al.* 2014). Meanwhile, animal experiments showed that the necroptosis inhibitor, Necrostatin-1, could exert efficient protection function against MIRI (Dmitriev *et al.* 2013). However, whether HSP70 inhibits necroptosis via suppressing autophagy during MIRI is unknown.

In this study, we aim to profile the relationship between HSP70, autophagy, and necroptosis during MIRI, demonstrating that HSP70 inhibits necroptosis through suppression of autophagy to promote cardiomyocyte survival. Hereon, we found a novel scenario on what exact functions HSP70 acts as a protective molecule during MIRI.

## Materials and Methods

**Animal experimental protocols** Sprague–Dawley (SD) rats, weight 230–280 g, were obtained from the Experimental Animal Center, Nantong University. All procedures were in accordance with the Guide for the Care of Use of Laboratory Animals published by the US National Institute of Health (NIH Publication No. 85–23, revised in 1996). The rats were randomly divided into eight groups ($n = 6$ in each group): sham group in which rats underwent operation without suture tie-down of the left anterior descending (LAD) coronary artery; experimental groups in which rats underwent ischemia for 30 min with 0, 2, 4, 6, 8, 12, or 24 h reperfusion, respectively.

**Surgery of animals** All animals were operated under anesthesia with chloral hydrate. After endotracheal intubation, the heart was rapidly exposed via a left thoracotomy. Then, a 6-0 polyproline ligature was placed under the left coronary artery (LCA). The ends of the tie were threaded through a small plastic tube to form a snare for reversible LCA occlusion. Myocardial ischemia was confirmed by a pale area below the suture and ST-T elevation shown in electrocardiogram (ECG). After ischemia, reperfusion was achieved by loosening the snare and characterized by rapid disappearance of cyanosis. Following the operation, the incisions were closed in layers. The chest and endotracheal tubes were removed. Room temperature was maintained at 37°C.

**Western blot analysis** Western blot was prepared with myocardial tissue after operation ($n = 6$ at each time point). Samples were isolated from approximately 0.1 g of myocardial tissue at different time points and minced with eye scissors on ice. Total myocardial tissue protein was then homogenized in lysis buffer and clarified by centrifugation at 13, 000 rpm for 15 min in a microcentrifuge at 4°C. The protein was separated by SDS-PAGE, transferred to PVDF membranes (Millipore; Billerica, MA) at 300 mA for appropriate timespan. Membranes were exposed for HSP70 (mouse, 1:800; Santa Cruz; Dallas, TX); glyceraldehyde 3-phosphate dehydrogenase (GAPDH) (rabbit, 1:800; Santa Cruz); receptor-interacting protein 1 (RIP1) (goat, 1:800; Santa Cruz); and LC3A/B (mouse, 1:1000; Cell signaling) antibodies overnight at 4°C. Then, HRP-conjugated secondary antibodies (1:1000; Southern-Biotech, Birmingham, AL) were added and incubated for 2 h at 37°C. Finally, membranes were analyzed by enhanced chemiluminescence system (ECL, Cell Signaling).

**Immunohistochemical analysis** After MIR, rat hearts were perfused with sterile saline and 4% formalin successively (Fisher Scientific, Fairlawn, NJ). Then, hearts were rapidly collected and immersion fixed in 10% formalin for 24 h. The sections were cut serially (5 μm). For immunohistochemical staining, the sections were boiled at 121°C for 20 min in 10 mM citrate buffer solution (pH 6.0) for antigen retrieval. Endogenous peroxidase activity was blocked by soaking in 0.3% hydrogen peroxide. After rinsing in PBS (pH 7.2), the sections were incubated with HSP70, RIP1, and LC3A/B antibodies for 2 h at 37°C. After incubation, the sections were washed with PBS for three times and incubated with secondary antibody for 30 and 20 min at 37°C separately. After three times washing by PBS, the sections were incubated with DAB in 0.05 mol/L Tris buffer (pH 7.6) containing 0.03% $H_2O_2$ for signal development. Finally, the slides were dehydrated, cleared, and cover slipped (Wang *et al.* 2012). All of analyses were conducted by Image-Pro plus 6.0 software.

**Isolation and culture of rat ventricular cardiomyocytes** Neonatal rat ventricular myocytes were isolated from 2-d-old SD rats. The hearts were collected, minced, and digested in trypsin. The primary neonatal rat cardiomyocytes were cultured in Dulbecco's modified Eagle's medium (DMEM) containing 15% fetal bovine serum (FBS). The medium was replaced with DMEM lacking FBS before the cells were placed into a hypoxic incubator (95% $N_2$, 5% $CO_2$, 37°C). After 6 h in the hypoxic incubator, cells were transferred to a normal incubator (21% $O_2$, 5% $CO_2$, 74%$N_2$, 37°C) for 6 h to reoxygenation (Ji *et al.* 2013).

**Double immunofluorescent staining** The primary cardiomyocytes were cultured in 24-wells plate (Corning Inc., Corning, NY). After H/R stimuli, the cells were fixed in 4% paraformaldehyde. All samples were incubated overnight at 4°C with primary antibody for HSP70 (1:100; Santa Cruz) and different markers as follows: α-actinin (cardiomyocyte marker, 1:100; Santa Cruz), RIP1 (1:100; Santa Cruz), and LC3A/B (1:100; cell signaling). After washing in PBS for three times, each time 15 min, a mixture of 4, 6-diamidino-2-phenylindole (DAPI) with FITC- and Cy3-conjugated secondary antibodies were added in a dark room and incubated overnight at 4°C. The stained sections were analyzed with a Leica fluorescence microscope (Leica DM 5000B, Germany).

**Small interfering RNA-based experiment** Three small interfering RNAs (siRNAs) targeting HSP70 gene were designed and synthesized by Shanghai Genepharma (Shanghai, China), and the most effective siRNA (siHSP70) identified by western blot was applied for sequent experiments. The sequences of three siHSP70s are as follows: 5′-GCUGAG AAAGAGGAGUUCGTT-3′, 5′-GAAUGCGCUC GAGUCCUAUTT-3′, 5′-GCUGAGAAAGAGG AGUUCGTT-3′. Scrambled RNA oligonucleotides were used as control. Twenty-four hours prior to transfection, cardiomyocytes were plated onto a 6-well plate (Corning Inc., Corning, NY) at 40–60% confluence. For each well, 33.3 nM siHSP70 or scrambled siRNA was transfected using Lipofectamine 2000 (Invitrogen, Carlsbad, CA) according to the manufacturer's instructions. The medium was replaced with DMEM containing 10% FBS after 6 h (Wan *et al.* 2015).

**Overexpression plasmid-based experiment** Overexpression plasmid of HSP70 was purchased from PPL plasmid library (Nanjing, Jiangsu, China). The transfection procedure was identical to siRNA transfection described above.

**LDH assay** The LDH assay kit was purchased from Jiancheng bioengineering institute (Nanjing, Jiangsu, China). All measurements were conducted following the instructions.

**Statistical assay** The SPSS19.0 software was used for statistical analysis. The results were presented as means ± SD. Differences between groups were calculated using the Student *t* test or one-way analysis of variance. $P < 0.05$ was considered statistically significant. All the experiments were repeated for at least three times with the consistent results.

## Results

**HSP70 expression is opposite to autophagy and necroptosis markers after MIRI** The rat myocardial IR model was constructed by temporarily occluding the LAD coronary artery, which was verified by ECG. Normal ECG was used as the negative control Fig. 1*A*. The changes of ST segment elevation and wide QRS waves were observed after myocardial ischemia immediately. With myocardial reperfusion, the electrophysiological changes indicated the recovery of cardiac function. However, reperfusion could not reverse the changes of ECG completely compared to the ischemia group, which showed the establishment of MIR Fig. 1*B*, *C*.

With the elongation of reperfusion, HSP70 expression increased immediately after MIR and peaked during 6 to 8 h. Afterwards, HSP70 expression decreased, while the ratio of LC3B to LC3A was increased rapidly during 12 h of reperfusion, and RIP1 expression showed a gradually increase from 4 h of reperfusion Fig. 1*D*. Interestingly, after 2 h reperfusion following ischemia, HSP70 expression was postponed after the blooming of autophagy, followed by the increase of RIP1 expression which indicated the initiation of necroptosis Fig.1*E*, *F*. These results suggested that HSP70 might be related to autophagy and necroptosis during MIR.

To identify the cellular location of HSP70, LC3A/B, and RIP1, we chose the notable time point, 6 h reperfusion after ischemia to perform the immunohistochemistry. It is shown that after MIR, HSP70 was located in the nucleus and cytoplasm of cardiomyocytes while RIP1 and LC3A/B were located predominately in the cytoplasm of cardiomyocytes Fig. 1*G*. Meanwhile, the analysis of positive cells showed the increase of HSP70, LC3A/B, and RIP1 expression following MIR Fig. 1*H*.

**HSP70 is associated with cardiomyocyte autophagy and necroptosis after MIRI** To mimic MIRI in vitro, we used the neonatal rat ventricular myocytes with H/R treatment. LDH release burst after hypoxia during 8 h reoxygenation. However, LDH release was blunt after 8 h reoxygenation, but reoxygenation could not completely reverse LDH release to normal level Fig. 2*A*. The HSP70, LC3A/B, and RIP1 expression showed similar change after H/R treatment compared with that of MIRI in vivo Fig. 2*B*, *C*, *D*. These results further suggested that HSP70 was associated with cardiomyocyte autophagy and necroptosis. In the consequent experiments, 6 h of reoxygenation after hypoxia and 6 h was set for H/R stimuli.

To further investigate the relationship among HSP70, autophagy, and necroptosis, we performed double immunofluorescence staining of HSP70, LC3A/B, and RIP1 in neonatal rat ventricular myocytes after H/R. It was obvious that HSP70, LC3A/B, and RIP1 co-localized in the cytoplasm of myocytes after 6 h reoxygenation Fig. 2*E*. These results further indicated that HSP70 was related to autophagy and necroptosis of cardiomyotes.

**The knockdown of HSP70 facilitates necroptosis and autophagy in cardiomyocytes after H/R treatment** To explore

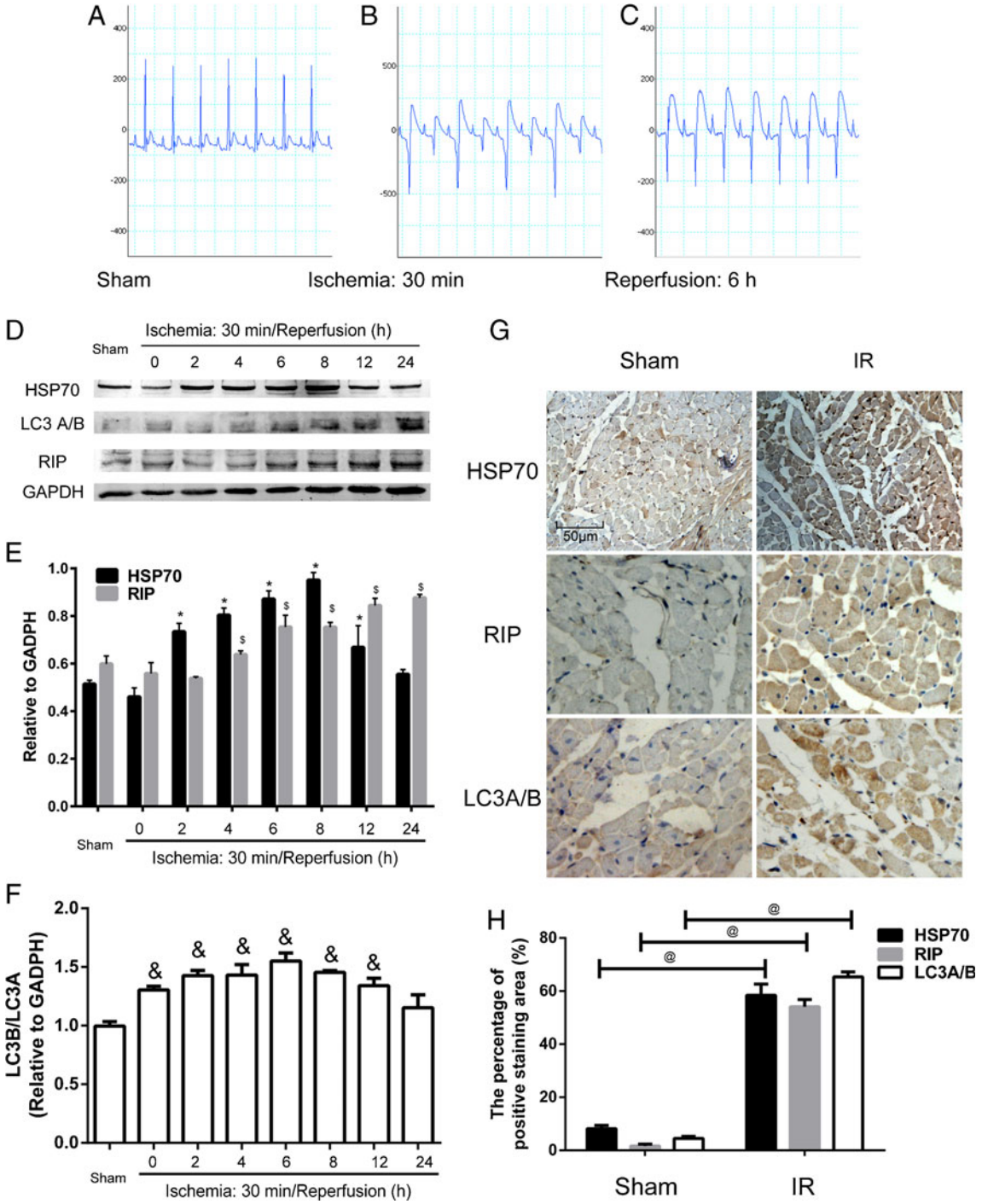


**Figure 1** HSP70 expression is opposite to autophagy and necroptosis markers after MIR in vivo. Adult SD rats were treated with ischemia for 30 min and different time points of reperfusion. *A* Normal ECG was taken as control. *B* ECG of acute myocardial ischemia. Marked ST-segment elevation was recorded, which indicated proximal occlusion of LAD artery. *C* ECG showed recovery of ST elevation and decrease in the T wave amplitude. *D* HSP70, LC3 A/B, and RIP1 expressions were detected by western blot after MIR. *E* Statistical graphs (relative optical density) show HSP70 and RIP1 expressions to GAPDH. *F* Statistical graph (relative optical density) shows the ratio of LC3B to LC3A. *G* Immunohistochemistry detected HSP70, LC3A/B, and RIP1. *Scale bars* = 50 μm in first image (applied to all). *H* Statistical graphs for the positive areas of tissues. *Asterisk*, *dollar sign*, *ampersand*, and *commercial at* represent $P < 0.05$ compared with the sham group.

the effects of HSP70 on autophagy and necroptosis, we utilized siRNA to downregulate HSP70 expression. The HSP70 siRNA3 could significantly downregulate HSP70 expression compared to scrambled siRNA, and the rescue experiments confirmed that HSP70 siRNA3 specifically downregulated HSP70 expression Fig. 3*A*. After transfected with siHSP70,

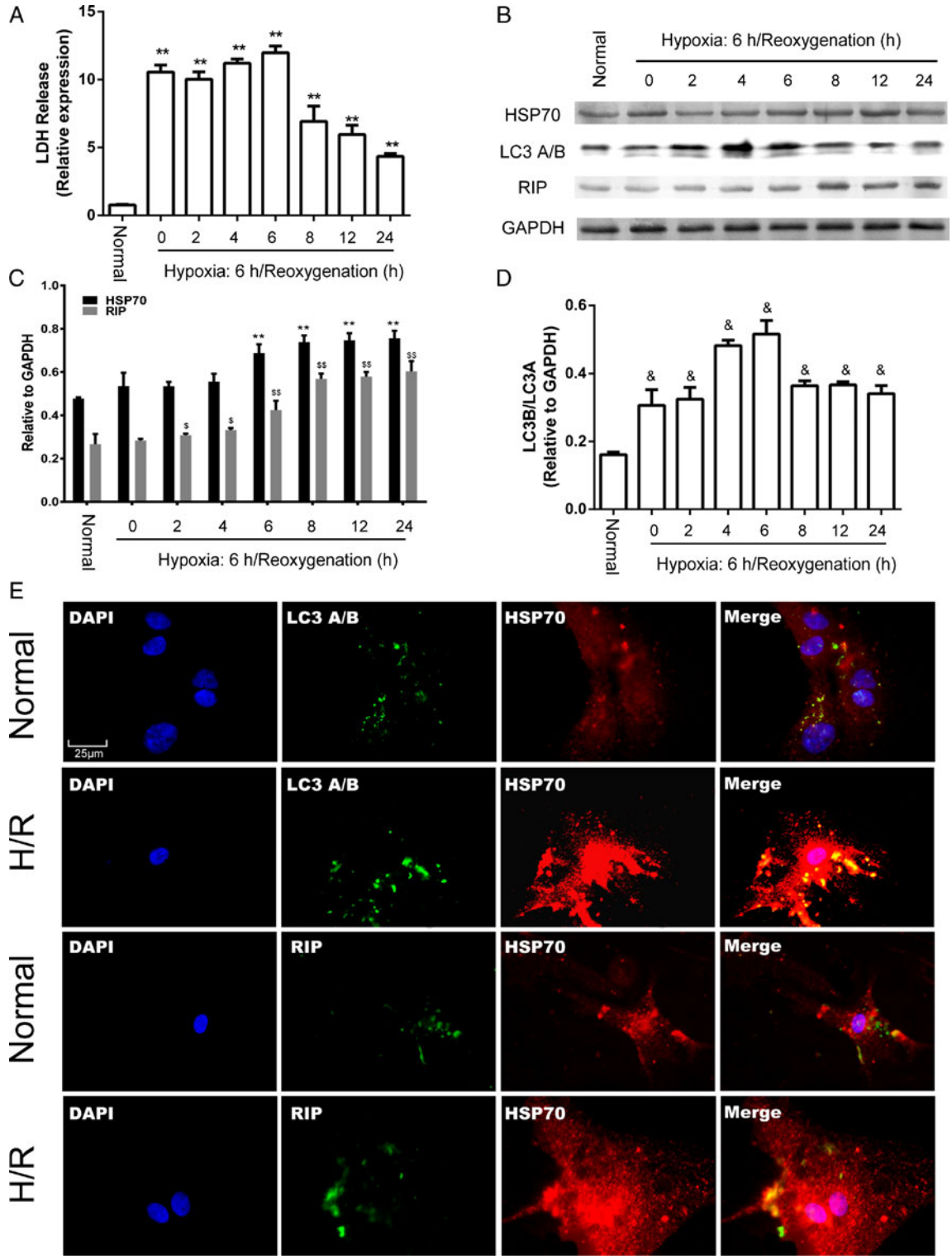


**Figure 2** HSP70 expression is opposite to autophagy and necroptosis markers in neonatal ventricular cardiomyocytes following H/R treatment in vitro. Neonatal ventricular cardiomyocytes were treated with 6 h hypoxia and different times of reoxygenation. *A* LDH assay was conducted to detect cell death. *B* HSP70, LC3 A/B, and RIP1 expressions were detected by western blot after H/R. *C* Statistical graph (relative optical density) shows HSP70 and RIP1 expressions to GAPDH. *D* Statistical graph (relative optical density) shows the ratio of LC3B to LC3A. *E* Distribution of HSP70 with LC3A/B and RIP1 with or without H/R. Neonatal ventricular cardiomyocytes fixed on the small plates were detected for HSP70, LC3A/B, and RIP1. DAPI was used to label nuclei (H/R: hypoxia for 6 h and reoxygenation for 6 h). *Scale bars* = 25 μm in first image (applied to all).

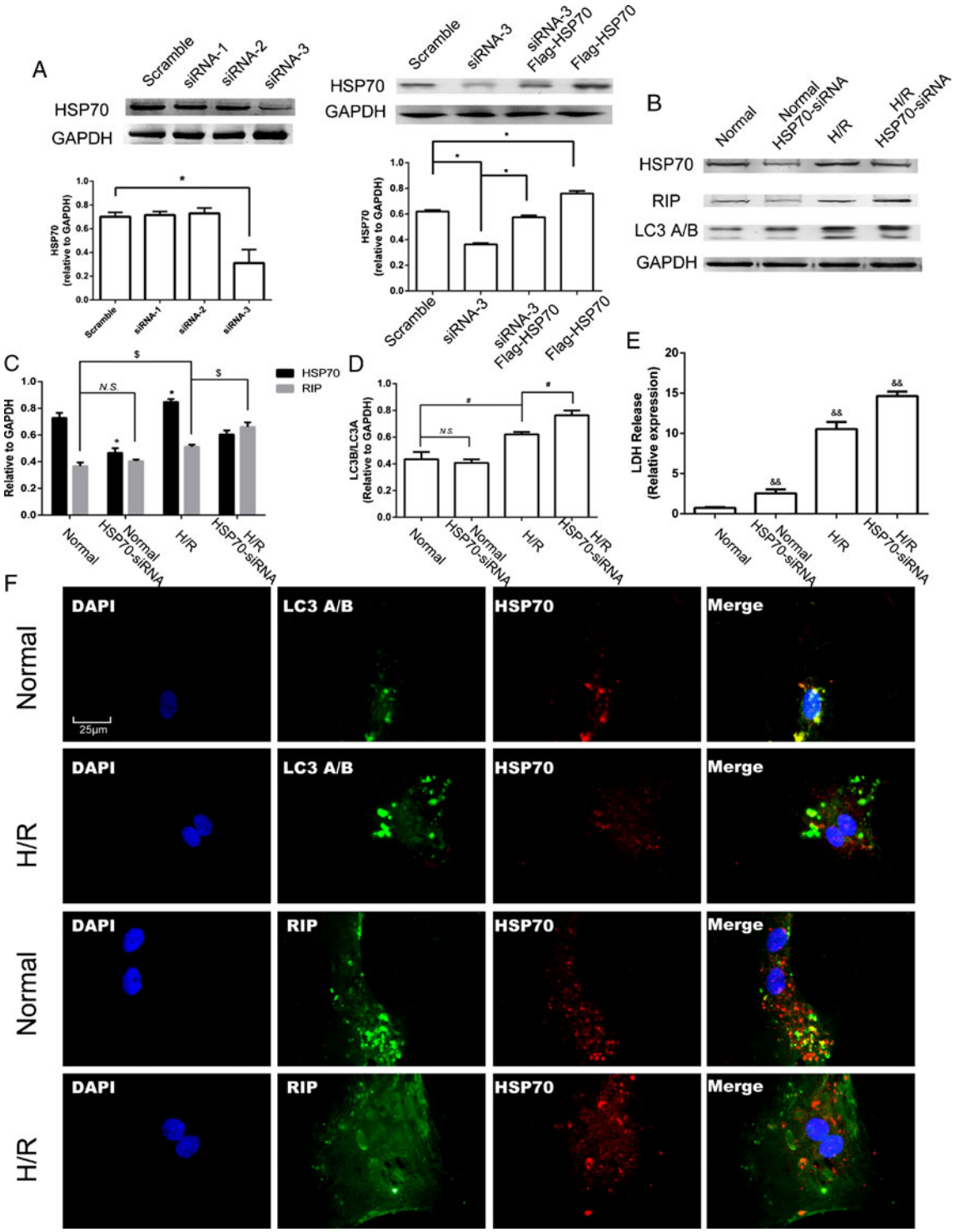


**Figure 3** HSP70 knockdown upregulates neonatal ventricular cardiomyocyte autophagy and necroptosis. Knocking down of HSP70 in neonatal ventricular cardiomyocytes with or without H/R. *A* HSP70 protein expression after HSP70 knockdown in cardiomyocytes with overexpression of HSP70 rescued. *B* HSP70, LC3 A/B, and RIP1 expressions were detected by western blot. *C* Statistical graph (relative optical density) shows HSP70 and RIP1 expressions to GAPDH. *D* Statistical graph (relative optical density) shows the ratio of LC3B to LC3A. *E* LDH assay was conducted to detect cell death. *F* Co-location of HSP70 with LC3A/B and RIP1 with or without H/R in neonatal ventricular cardiomyocytes after HSP70 knockdown. Neonatal ventricular cardiomyocytes fixed on the small plates were detected for HSP70, LC3A/B, and RIP1. DAPI was used to label nuclei (H/R: hypoxia for 6 h and reoxygenation for 6 h). *Scale bars* = 25 μm in first image (applied to all).

HSP70 expression was downregulated in normal group and H/R group, respectively Fig. 3*B*. However, the ratio of LC3B to LC3A and RIP1 expression were upregulated following H/R. Interestingly, the changes did not appear in the normal groups Fig. 3*C*, *D*. While LDH assay showed that HSP70 knockdown led to increasing cell death after H/R Fig. 3*E*.

To clarify the changes of distribution and expression of LC3A/B and RIP1 after HSP70 knockdown, double immunofluorescence staining was carried out. After HSP70 knockdown, autophagy and necroptosis were upregulated in cadiomyocytes following H/R stimuli, while the cells without H/R stimuli had no obvious changes of autophagy and necroptosis Fig. 3*F*. These results indicated that HSP70 only had effects on cardiomyocytes after H/R stimuli.

**HSP70 inhibits cardiomyocyte necroptosis via suppressing autophagy** After given z-VAD-FMK (an apoptosis inhibitor, 50 μM for 1 h), the cardiomyocytes were selectively treated with 3-MA (an autophagy inhibitor, 5 mM for 2 h), rapamycin (an autophagy activator, 0.5 μM for 4 h), and necrostatin-1 (a necroptosis inhibitor, 50 μM for 2 h) and transfected with siHSP70. When autophagy or necroptosis was inhibited, HSP70 expression did not change obviously. However, when autophagy was inhibited, RIP1 expression was downregulated. Additionally, the autophagy inhibitor could abolish the increased expression of RIP1 caused by siHSP70 transfection. Meanwhile, rapamycin caused further increase of RIP1 expression which was in relevance with siHSP70 transfection Fig. 4*A*-*C*.

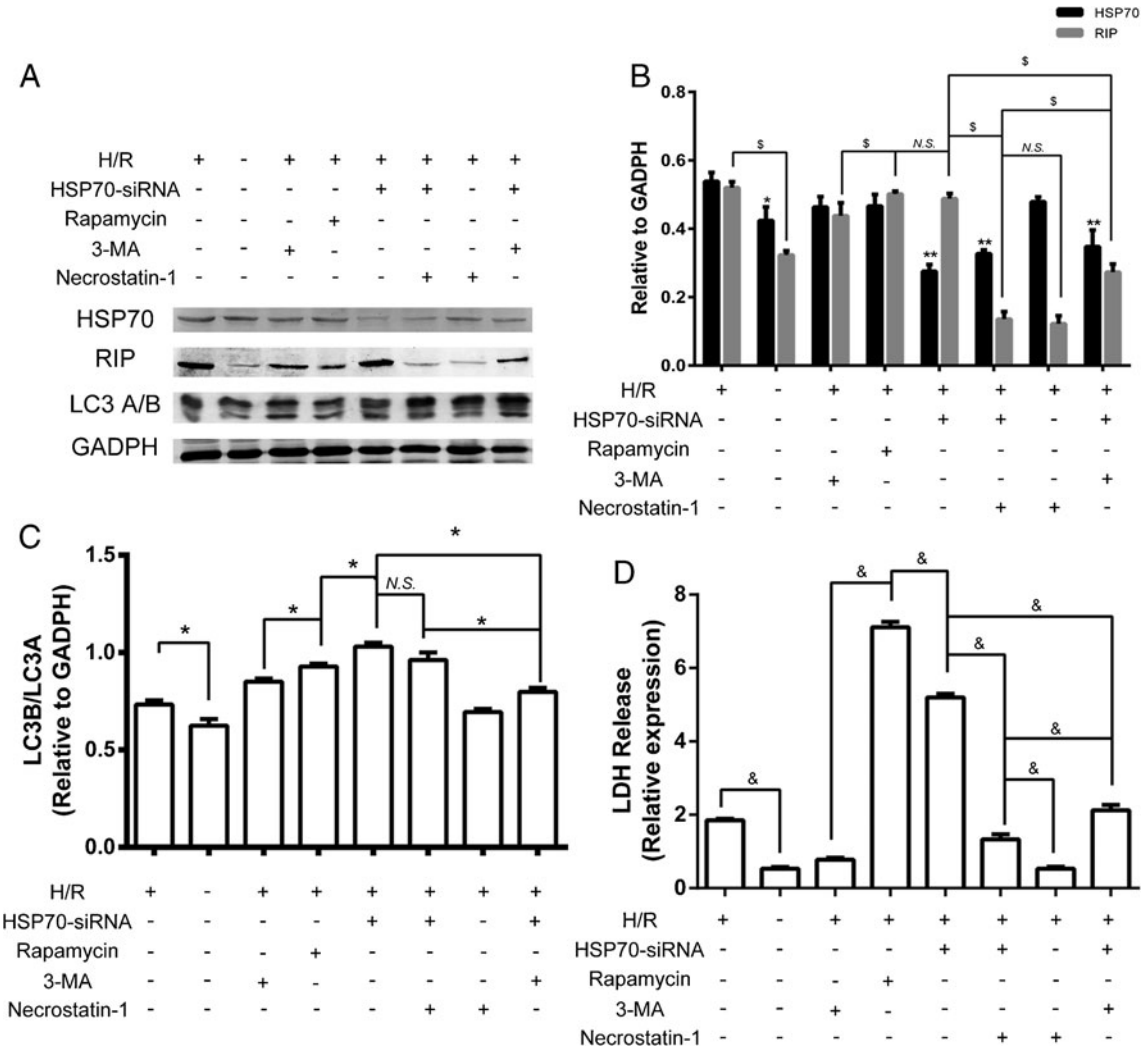


**Figure 4** HSP70 inhibits cardiomyocyte necroptosis via suppressing autophagy. After given z-VAD-FMK, an apoptosis inhibitor, cardiomyocytes were selectively treated with 3-MA (an autophagy inhibitor), rapamycin (an autophagy activator), and necrostatin-1 (a necroptosis inhibitor) and transfected with siHSP70. *A* HSP70, LC3 A/B, and RIP1 expressions were detected by western blot. *B* Statistical graph (relative optical density) shows HSP70 and RIP1 expressions to GAPDH. *C* Statistical graph (relative optical density) shows the ratio of LC3B to LC3A. *D* LDH assay was conducted to detect cell death.

Ultimately, we used LDH assay to detect cell damage, showing that HSP70 knockdown resulted in more cell damage compared to cardiomyocytes exposed to autophagy and necroptosis inhibitor. Interestingly, after siHSP70 transfection, autophagy inhibitor exerted a stronger effect of alleviating cell damage compared to cardiomyocytes given necroptosis inhibitor only Fig. 4*D*. Herein, these results suggested that HSP70 inhibited necroptosis and autophagy, while inhibition of autophagy had effects on necroptosis,

## Discussion

Over the past decade, the treatment for acute myocardial ischemia diseases has enjoyed significant advances, especially the therapies for ST-segment elevation myocardial infarction (STEMI). However, STEMI still has high morbidity and mortality worldwide (Windecker *et al.* 2013). The main reason that blocks myocardial recovery from ischemia diseases is MIRI (Bagai *et al.* 2014). Recently, autophagy has been regarded as a novel pathophysiological process during MIR, which is of great significance besides apoptosis and creates a scenario of both pros and cons (Gottlieb and Mentzer 2010). However, more researches showed that inhibition of autophagy could reduce cell death after H/R stimuli in cardiomyocytes, while lysosomal degradative pathway activation which was characterized by the ratio of LC3B/LC3A after MIR was aggressive to promote cardiomyocyte death (Gurusamy *et al.* 2009; Wang *et al.* 2015). In our study, after 2 h reperfusion, autophagy was promoted and prolonged for the next 10 h, which was in line with the previous studies (Jian *et al.* 2015; Xiao *et al.* 2015).

Necroptosis, a programmed cell necrosis, leads to a reduction of cardiac function (Koshinuma *et al.* 2014). RIP1 is one of the representatives for the activation of necroptosis (Rosentreter *et al.* 2015). Autophagy could promote both necroptosis and apoptosis in human glioblastoma cells in vitro (Zhang *et al.* 2015). Herein, we used rat MIR and neonatal cardiomyocyte H/R models to detect autophagy and necroptosis, finding 6 h reoxygenation time point showed great changes and autophagy occurred before necroptosis initiated, suggesting that autophagy triggered necroptosis. Furthermore, in renal IR, HSP70 exerted a protective effect through suppressing autophagy (Yeh *et al.* 2010). In present study, after HSP70 knockdown, autophagy and necroptosis were activated following cardiomyocyte H/R stimuli, which was in line with the previous research (Huang *et al.* 2013).

Regulated autophagy could protect cells against death (Huang *et al.* 2015). However, MIR leads to excessive autophagy activation, which results in organelle damage, cellular dysfunction, and cell death (Levine and Yuan 2005). As excessive autophagy triggers apoptosis and necroptosis during MIR, we utilized z-VAD-FMK, a pan-caspase inhibitor to block apoptosis. Furthermore, autophagy activator rapamycin and autophagy inhibitor 3-MA, necroptosis inhibitor necrostatin-1 were applied. The autophagy activator could exert similar effect on cardiomyocytes as HSP70 knockdown, which could promote autophagy and cell death (Xiao *et al.* 2015). Moreover, with HSP70 knockdown in vitro, autophagy inhibitor could still block necroptosis, indicating that HSP70 was not the only regulator of autophagy, which was consistent as previously reported (Wei *et al.* 2015). In line with previous researches (Dmitriev *et al.* 2015), after HSP70 knockdown, necroptosis inhibitor had no effect on autophagy. Thereafter, necroptosis inhibitor was not capable to downregulate cell death as autophagy inhibitor, indicating besides caspase-dependent apoptosis, caspase-independent apoptosis also participated in cell death, which was in parallel with the previous study (Anitha *et al.* 2014). However, HSP70 knockdown promoted more cell death than autophagy activator, suggesting that HSP70 had other protective functions during MIR as previously reported (Peng *et al.* 2010; Vicencio *et al.* 2015). In summary, HSP70 attenuated necroptosis of cardiomyocytes via suppressing autophagy after MIR.

Our study has several limitations that need to be mentioned. Firstly, as the ratio of LC3B to LC3A represented macroautophagy, knockdown of HSP70 also affects chaperone-mediated autophagy during MIR, which needs more investigation. Secondly, whether HSP70 and autophagy affect other necroptosis-associated molecules such as RIP13, A20 needs further study.

**Acknowledgments** This work was supported in part by the National Natural Science Foundation of China (Nos. 81401365, 81373223, 81200918, 81172879), a project funded by the Priority Academic Program Development of Jiangsu Higher Education Institutions (PAPD); Nantong science and technology project (MS12015056); Nantong University graduate scientific and technological innovation projects (No. YKS14010).

**Compliance with ethical standards**

**Conflict of interest** The authors declare that they have no conflict of interest.

## References

Anitha J, Pradeep AR, Sivaprasad V (2014) Upregulation of Atg5 and AIF gene expression in synchronization with programmed cellular death events in integumental epithelium of Bombyx mori induced by a dipteran parasitoid infection. Bull Entomol Res 104:794–800

Bagai A, Dangas GD, Stone GW, Granger CB (2014) Reperfusion strategies in acute coronary syndromes. Circ Res 114:1918–1928

Dannappel M, Vlantis K, Kumari S, Polykratis A, Kim C, Wachsmuth L, Eftychi C, Lin J, Corona T, Hermance N, Zelic M, Kirsch P, Basic M, Bleich A, Kelliher M, Pasparakis M (2014) RIPK1 maintains

epithelial homeostasis by inhibiting apoptosis and necroptosis. Nature 513:90–94

Dmitriev YV, Minasian SM, Demchenko EA, Galagudza MM (2013) Study of cardioprotective effects of necroptosis inhibitors on isolated rat heart subjected to global ischemia-reperfusion. Bull Exp Biol Med 155:245–248

Dmitriev YV, Minasyan SM, Vasina LV, Demchenko EA, Galagudza MM (2015) Effects of inhibitors of necroptosis and autophagy on morphofunctional characteristics of the myocardium during static cold storage of donor rat heart. Bull Exp Biol Med 159:792–795

Feng Y, Huang W, Meng W, Jegga AG, Wang Y, Cai W, Kim HW, Pasha Z, Wen Z, Rao F, Modi RM, Yu X, Ashraf M (2014) Heat shock improves Sca-1+ stem cell survival and directs ischemic cardiomyocytes toward a prosurvival phenotype via exosomal transfer: a critical role for HSF1/miR-34a/HSP70 pathway. Stem Cells 32:462–472

Garrido C, Brunet M, Didelot C, Zermati Y, Schmitt E, Kroemer G (2006) Heat shock proteins 27 and 70: anti-apoptotic proteins with tumorigenic properties. Cell Cycle 5:2592–2601

Gottlieb RA, Mentzer RM (2010) Autophagy during cardiac stress: joys and frustrations of autophagy. Annu Rev Physiol 72:45–59

Gottlieb RA, Finley KD, Mentzer RM Jr (2009) Cardioprotection requires taking out the trash. Basic Res Cardiol 104:169–180

Gurusamy N, Lekli I, Gorbunov NV, Gherghiceanu M, Popescu LM, Das DK (2009) Cardioprotection by adaptation to ischaemia augments autophagy in association with BAG-1 protein. J Cell Mol Med 13: 373–387

Hsu SF, Chao CM, Huang WT, Lin MT, Cheng BC (2013) Attenuating heat-induced cellular autophagy, apoptosis and damage in H9c2 cardiomyocytes by pre-inducing HSP70 with heat shock preconditioning. Int J Hyperth: Off J Eur Soc Hyperth Oncol, N Am Hyperth Group 29:239–247

Huang CY, Kuo WT, Huang YC, Lee TC, Yu LC (2013) Resistance to hypoxia-induced necroptosis is conferred by glycolytic pyruvate scavenging of mitochondrial superoxide in colorectal cancer cells. Cell Death Dis 4, e622

Huang Z, Han Z, Ye B, Dai Z, Shan P, Lu Z, Dai K, Wang C, Huang W (2015) Berberine alleviates cardiac ischemia/reperfusion injury by inhibiting excessive autophagy in cardiomyocytes. Eur J Pharmacol 762:1–10

Ji L, Li H, Gao P, Shang G, Zhang DD, Zhang N, Jiang T (2013) Nrf2 pathway regulates multidrug-resistance-associated protein 1 in small cell lung cancer. PLoS One 8, e63404

Jian J, Xuan F, Qin F, Huang R (2015) Bauhinia championii flavone inhibits apoptosis and autophagy via the PI3K/Akt pathway in myocardial ischemia/reperfusion injury in rats. Drug Des, Dev Ther 9: 5933–5945

Jiang H, Xiao J, Kang B, Zhu X, Xin N, Wang Z (2015) PI3K/SGK1/GSK3beta signaling pathway Is involved in inhibition of autophagy in neonatal rat cardiomyocytes exposed to hypoxia/reoxygenation by Hydrogen sulfide. Exp Cell Res. doi:10.1016/j.yexcr.2015.07.005

Koshinuma S, Miyamae M, Kaneda K, Kotani J, Figueredo VM (2014) Combination of necroptosis and apoptosis inhibition enhances cardioprotection against myocardial ischemia-reperfusion injury. J Anesth 28:235–241

Levine B, Yuan J (2005) Autophagy in cell death: an innocent convict? J Clin Invest 115:2679–2688

Matsushima S, Tsutsui H, Sadoshima J (2014) Physiological and pathological functions of NADPH oxidases during myocardial ischemia-reperfusion. Trends Cardiovasc Med 24:202–205

Murphy E, Steenbergen C (2008) Mechanisms underlying acute protection from cardiac ischemia-reperfusion injury. Physiol Rev 88:581–609

Peng W, Zhang Y, Zheng M, Cheng H, Zhu W, Cao CM, Xiao RP (2010) Cardioprotection by CaMKII-deltaB is mediated by phosphorylation of heat shock factor 1 and subsequent expression of inducible heat shock protein 70. Circ Res 106:102–110

Rafiq K, Kolpakov MA, Seqqat R, Guo J, Guo X, Qi Z, Yu D, Mohapatra B, Zutshi N, An W, Band H, Sanjay A, Houser SR, Sabri A (2014) c-Cbl inhibition improves cardiac function and survival in response to myocardial ischemia. Circulation 129:2031–2043

Rani N, Bharti S, Manchanda M, Nag TC, Ray R, Chauhan SS, Kumari S, Arya DS (2013) Regulation of heat shock proteins 27 and 70, p-Akt/p-eNOS and MAPKs by Naringin Dampens myocardial injury and dysfunction in vivo after ischemia/reperfusion. PLoS One 8, e82577

Rosentreter D, Funken D, Reifart J, Mende K, Rentsch M, Khandoga A (2015) RIP1-dependent programmed necrosis is negatively regulated by caspases during hepatic ischemia-reperfusion. Shock 44:72–76

Sun L, Fan H, Yang L, Shi L, Liu Y (2015) Tyrosol prevents ischemia/reperfusion-induced cardiac injury in H9c2 cells: involvement of ROS, Hsp70, JNK and ERK, and apoptosis. Molecules 20:3758–3775

Vander Heide RS, Steenbergen C (2013) Cardioprotection and myocardial reperfusion: pitfalls to clinical application. Circ Res 113:464–477

Vicencio JM, Yellon DM, Sivaraman V, Das D, Boi-Doku C, Arjun S, Zheng Y, Riquelme JA, Kearney J, Sharma V, Multhoff G, Hall AR, Davidson SM (2015) Plasma exosomes protect the myocardium from ischemia-reperfusion injury. J Am Coll Cardiol 65:1525–1536

Wan C, Hou S, Ni R, Lv L, Ding Z, Huang X, Hang Q, He S, Wang Y, Cheng C, Gu XX, Xu G, Shen A (2015) MIF4G domain containing protein regulates cell cycle and hepatic carcinogenesis by antagonizing CDK2-dependent p27 stability. Oncogene 34:237–245

Wang Y, Yang S, Ni Q, He S, Zhao Y, Yuan Q, Li C, Chen H, Zhang L, Zou L, Shen A, Cheng C (2012) Overexpression of forkhead box J2 can decrease the migration of breast cancer cells. J Cell Biochem 113:2729–2737

Wang B, Zhong S, Zheng F, Zhang Y, Gao F, Chen Y, Lu B, Xu H, Shi G (2015) N-n-butyl haloperidol iodide protects cardiomyocytes against hypoxia/reoxygenation injury by inhibiting autophagy. Oncotarget 6:24709–24721

Wei P, Yang XJ, Fu Q, Han B, Ling L, Bai J, Zong B, Jiang CY (2015) Intermedin attenuates myocardial infarction through activation of autophagy in a rat model of ischemic heart failure via both cAMP and MAPK/ERK1/2 pathways. Int J Clin Exp Pathol 8:9836–9844

Whelan RS, Kaplinskiy V, Kitsis RN (2010) Cell death in the pathogenesis of heart disease: mechanisms and significance. Annu Rev Physiol 72:19–44

Windecker S, Bax JJ, Myat A, Stone GW, Marber MS (2013) Future treatment strategies in ST-segment elevation myocardial infarction. Lancet 382:644–657

Xiao J, Zhu X, Kang B, Xu J, Wu L, Hong J, Zhang Y, Ni X, Wang Z (2015) Hydrogen sulfide attenuates myocardial hypoxia-reoxygenation injury by inhibiting autophagy via mTOR activation. Cell Physiol Biochem: Int J Exp Cell Physiol, Biochem, Pharmacol 37:2444–2453

Yeh CH, Hsu SP, Yang CC, Chien CT, Wang NP (2010) Hypoxic preconditioning reinforces HIF-alpha-dependent HSP70 signaling to reduce ischemic renal failure-induced renal tubular apoptosis and autophagy. Life Sci 86:115–123

Zhang L, Wang H, Ding K, Xu J (2015) FTY720 induces autophagy-related apoptosis and necroptosis in human glioblastoma cells. Toxicol Lett 236:43–59